Organic Process Research & Development **2008,** *12,* 264–270

Effect of Water Activity on the Transformation between Hydrate and Anhydrate of Carbamazepine

Yi Li,*[,†] Pui Shan Chow,[†] Reginald B. H. Tan,[†,‡] and Simon N. Black[§]

*Institute of Chemical and Engineering Sciences, A*STAR (Agency for Science, Technology and Research), 1 Pesek Road, Jurong Island, Singapore 627833, Department of Chemical and Biomolecular Engineering, National University of Singapore, 4 Engineering Drive 4, Singapore 117576, and AstraZeneca, Macclesfield SK10 2NA, England*

Abstract:

Pharmaceutical hydrates have substantial impact on the bioavailability of drugs, and controlling the formation of hydrates is of significant importance in the pharmaceutical crystallization and formulation processes. The relative stability of carbamazepine anhydrate (CBZA) and dihydrate (CBZD) at room temperature was investigated by using slurry experiments. Optical microscopy, powder X-ray diffraction, Karl Fischer titration, thermogravimetric analysis, and differential scanning calorimetry were used to characterize CBZA and CBZD. The results of slurry experiments showed that the water content at equilibrium plays a vital role in determining the relative stability of CBZA and CBZD. At 20 °C, CBZD is more stable than CBZA when the water content of the solvent mixture in equilibrium (C_{we}) is higher than 19.6%, and vice versa. It was also found that CBZD and CBZA can coexist in equilibrium when C_{we} is equal to 19.6% or water activity of 0.636 at 20 °C. The three-component phase diagram was established for better understanding of the relationship between the water content and the relative stability of CBZD and CBZA. The compositions at which CBZD and CBZA can coexist at high CBZ content can be displayed usefully by the three-component phase diagram. This demonstrates the importance of three-component phase diagrams for analyzing the relative stability of pharmaceutical anhydrates and hydrates.

Introduction

Many pharmaceutical compounds can exist in both anhydrous and hydrated forms. *The European Pharmacopei*a in 1991 showed that 57% of pharmaceutical compounds were capable of forming hydrates.[1] Pharmaceutical hydrates can be formed when contacted with water or water vapor during crystallization, lyophilization, wet granulation, aqueous film coating, spray drying, and storage. The presence of water molecules within the crystal lattice of pharmaceutical compounds affects packing arrangements of molecules, intermolecular interactions, and crystalline disorder, and hence influences solubility, dissolution rate, stability, and bioavailability of pharmaceutical materials.[2] The potential impact of such changes in the hydration state of pharmaceutical compounds is substantial throughout the drug development process. It is therefore vital to understand and control the anhydrate−hydrate phase transformation of pharmaceutical compounds to ensure that unexpected phase changes do not happen during the production and storage of the product.

Although it is not essential, the preference is to develop the pure thermodynamically stable crystal forms over the temperature/relative humidity range to which pharmaceutical compounds will be subjected. Understanding the relative stability of polymorphs and hydrates is the prerequisite of finding the optimum solid forms in drug development. Crystallizations resulting in mixtures of polymorphs (sometimes called "concomitant polymorphs")[3] are usually understood not to have reached thermodynamic equilibrium. In such cases, maintaining mixtures of polymorphs in solvents long enough eventually results in isolation of one stable form.[4] Such experiments, known as "slurry experiments", have become very common in the pharmaceutical industry to assess the relative stability of polymorphs. As the relative thermodynamic stability of polymorphs varies with temperature and pressure,[5] changing solvent compositions does not alter their relative thermodynamic stability. Therefore, theoretically the most stable polymorph can always be obtained through slurry experiments, regardless the composition of solvents or solvent mixture.

In contrast, the hydration state of the pharmaceutical compounds is dependent on solvent composition. Recently, slurry experiments studying the thermodynamic equilibrium between the hydrate and the anhydrous forms of theophylline,[6,7] ampicillin,[8] and quinolones[9] in water−solvent mixture demonstrated that the water activity in mixed solvents is the major factor in determining the hydration state of drugs. Recently, Black et al.[10] and Variankaval et al.[11] observed that some isolated samples were physical mixtures of hydrate and anhy-

* Corresponding author. Telephone: (65)6796-3860. Fax: (65)6316-6183. E-mail: Li_Yi@ices.a-star.edu.sg.

† A*STAR.

‡ National University of Singapore.

§ AstraZeneca.

(1) Bechtloff, B.; Nordhoff, S.; Ulrich, J. *Cryst. Res. Technol.* **2001**, *36*, 1315–1328.

(2) Khankari, R. K.; Grant, D. J. W. *Thermochim. Acta* **1995**, *248*, 61–79.

(3) Bernstein, J.; Davey, R. J.; Henck, J. O. *Angew. Chem., Int. Ed.* **1999**, *38*, 3441–3461.

(4) Davey, R. J.; Blagden, N.; Righini, S.; Alison, H.; Ferrari, E. S *J. Phys. Chem. B* **2002**, *106*, 1954–1959.

(5) Brittain, H. G. *Polymorphism in Pharmaceutical Solids*; Mercel Dekker, Inc.: New York, 1999.

(6) Ticehurst, M. D.; Storey, R. A.; Watt, C. *Int. J. Pharm.* **2002**, *247*, 1–10.

(7) Zhu, H. J.; Yuen, C. M.; Grant, D. J. W. *Int. J. Pharm.* **1996**, *135*, 151–160.

(8) Zhu, H. J.; Grant, D. J. W. *Int. J. Pharm.* **1996**, *139*, 33–43.

(9) Romero, S.; Bustamante, P.; Escalera, B.; Mura, P.; Cirri, M. *J. Pharm. Biomed. Anal.* **2004**, *35*, 715–726.

(10) Black, S. N.; Cuthbert, M. W.; Roberts, R. J.; Stensland, B. *Cryst. Growth Des.* **2004**, *4*, 539–544.

(11) Variankaval, N.; Lee, C.; Xu, J.; Calabria, R.; Tsou, N.; Ball, R. *Org. Process Res. Dev.* **2007**, *11*, 229–236.

10.1021/op7001497 CCC: $40.75
Published on Web 03/05/2008

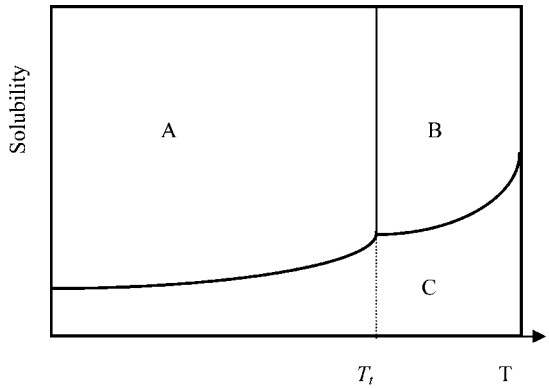

Figure 1. **Phase diagram for enantiotropic polymorphs.**

drate. This suggests that hydrates and anhydrates can coexist thermodynamically, whereas "true" polymorphs cannot. In order to better understand the difference between polymorphs and hydrates, the phase rule and phase diagram will be applied in the following theoretical section.

Theoretical Section

Figure 1 shows a phase diagram for a solvent and a material that has two polymorphs (not solvates or hydrates), which are enantiotropically related. Slurry experiments performed below the transition temperature T_t will eventually give Form A. Slurry experiments performed above T_t will eventually give Form B. Such slurry experiments can be used to establish the relative stability of polymorphs, and identify T_t. Although the solubilities of the two polymorphs will change with solvents, T_t does not.

The phase rule can be used to justify this approach. The phase rule states that:

$$F = C - P + 2 \tag{1}$$

where F is the degrees of freedom, C is the number of components, and P is the number of phases. When pressure is constant, the "reduced"-phase rule can be applied excluding the effect of pressure:

$$F' = C - P + 1 \tag{2}$$

where F' is the degrees of freedom, not including pressure.

In the case shown in Figure 1, there are two components (solvent and solute), and the pressure is constant, so eq 2 becomes

$$F' = 3 - P \tag{3}$$

Therefore when three phases (two polymorphs and the saturated solution) coexist, F' is equal to zero and the system is invariant. This corresponds to the point on the phase diagram where the vertical line above T_t intersects the solubility curve, and the temperature and the composition of the system are both fixed. In practice it is unlikely that these conditions will be found without prior knowledge, and therefore it is extremely unlikely that two solid phases will coexist in slurry experiments.

However, the situation will change completely when hydrates are formed in a mixed-solvent system. The above analysis no longer applies as an additional component; the second solvent, needs to be considered. In this case, the number of components is three: solute and two solvents. Hydrate and anhydrate together are considered one component because the composition of any phase can be expressed in terms of the anhydrate and water. At constant pressure, the reduced-phase rule becomes:

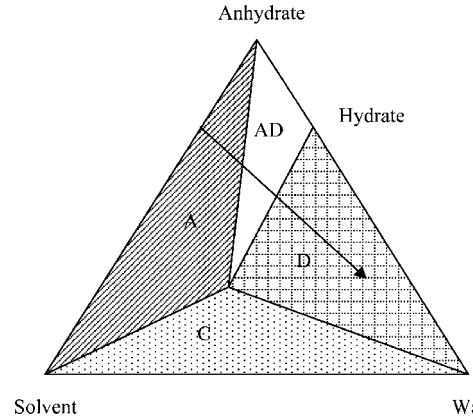

Figure 2. **Schematic, isothermal triangular phase diagram.**

$$F' = 4 - P \tag{4}$$

When hydrate and anhydrate coexist, there are in total three phases: two solid phases and one liquid phase (the two solvents are completely miscible). F' becomes one which means that hydrate and anhydrate continue to coexist in a range of temperatures rather than a fixed temperature as in the case of enantiotropic polymorph. As it is no longer possible to use two-dimensional solubility curves to represent the phase behavior of three-component systems, isothermal triangular phase diagrams are applied to display such information. Figure 2 shows such a diagram for a system in which both anhydrate and hydrate forms exist, and there are two solvents, one of which is water. Region C is where only solution phase exists, regions A and D are where only slurries of anhydrate and hydrate exist, respectively, and region AD is where anhydrate and hydrate coexist.

Consider the path represented by the arrow starting on the left-hand side of the triangle. This represents slurry of anhydrate in the second solvent, to which water is added. Initially the added water stays in solution, and there is only one solid phase. Eventually there will be sufficient water in solution to allow the hydrate to start crystallizing. As more water is added, the anhydrate converts to the hydrate, while the solution composition remains unchanged (region AD). Once all the anhydrate has disappeared, the water content in solution will start increasing again. One feature of such systems, readily apparent from Figure 2, is that the size (hence, the ease of detection) of the AD region is related to the weight percentage of water in the hydrate. In a previous study, the weight percentage of water in piperidine hydrate was 4.17%.[10] In contrast, carbamazepine (CBZ) dihydrate contains 13.2% of water in weight. Hence, CBZ/water/ethanol was chosen as the model system for this study.

Carbamazepine (CBZ), an antiepileptic drug, has been widely used for more than 20 years.[12] To date, four anhydrous polymorphs, a dihydrate, and several solvates have been reported.[13–15] Commercial tablets of CBZ are formulated with the monoclinic anhydrous form (CBZA) which is the most stable and least soluble of all anhydrous forms. However, CBZA transforms into dihydrate (CBZD) at high humidity[16] and in aqueous suspension.[17–19] Solubility data for CBZA and CBZD in ethanol–water systems at a variety of temperatures have also been reported,[20] but there were no examples of the thermodynamically stable coexistence of both crystal modifications, and their respective system compositions were not reported.

The aims of the present study were to investigate the thermodynamic stability of CBZA and CBZD in water−ethanol mixture using slurry experiments and establish a meaningful three-component phase diagram of carbamazepine. This work also demonstrates the importance of understanding phase equilibrium of a three-phase system through a three-component phase diagram, the usefulness of which has often been overlooked.

Experimental Section

2.1. Materials. Carbamazepine (BP98, monoclinic form) obtained from Suzhou Sintofarm Pharmaceutical of Feedstock Co. Ltd., Jiangsu, China, was used as raw material. Ethanol used was of analytical grade (Merck). Water used was of ultrapure grade (Millipore).

2.2. Preparation of Pure Form of CBZA and CBZD. CBZA was prepared by dissolving 25.5 g of CBZ raw material in 500 mL of ethanol. The solution was heated to 65 °C and held for 40 min to ensure complete dissolution of the CBZ crystals. It was then cooled to 20 °C at 1 °C/min and held at 20 °C for 5 h. CBZA that crystallized from the solution was finally filtered and dried overnight at 30 °C in a vacuum oven. The dried CBZA was stored in a desiccator at 30% relative humidity (RH).

CBZD was prepared by dissolving 25.5 g of CBZ raw material in 500 mL of 50% (v/v) water−ethanol mixture at 65 °C. The solution was cooled to 20 °C at a rate of 1 °C/min and held for 5 h. CBZD crystallized from the solution, was then filtered, and was dried overnight at 30 °C in a vacuum oven. The dried CBZD was stored at ambient temperature and 70% RH.

The products from the above crystallizations were characterized using powder X-ray diffraction (PXRD), thermogravimetric analysis (TGA) and differential scanning calorimetry (DSC) to confirm that they were indeed CBZA and CBZD as intended.

2.3. Slurry Experiment. Water−ethanol mixtures of varying water contents were prepared. An excess of CBZA and/or CBZD of known weight was added to the water−ethanol mixture in conical flasks. The suspensions were stirred at room temperature (20 °C) continuously for up to 14 days in order to attain thermodynamic equilibrium. Saturated solution samples were withdrawn by syringe, and passed through 0.2 μm membrane filters to remove suspended particles. The CBZ concentrations in saturated solution were determined by high performance liquid chromatography (HPLC) analysis, and water contents in saturated solutions were measured by Karl Fisher titration. Excess solids equilibrated with saturated solutions were collected by filtration, and then characterized by optical microscopy, PXRD, TGA, and DSC.

2.4. Characterization Methods. The concentration of carbamazepine was analyzed by an Agilent 1100 HPLC system. The reverse-phase column was a ZORBAX Extend-C18 column (4.6 mm × 150 mm with particle size of 3.5 μm). The mobile phase consisted of 45% methanol and 55% ultrapure water. The flow rate of the mobile phase was 1.0 mL/min. The absorbance was measured at 210 nm. PXRD patterns were analyzed with a Bruker D8-ADVANCE X-ray diffractometer (Co Kα radiation). The voltage and current applied were 40 kV and 40 mA respectively. The scan range was from 5° to 30° 2θ with a scanning rate of 0.02°/s. Single crystal X-ray measurements of CBZD were performed on a Rigaku Saturn 70 CCD area-detector diffractometer at 110 K with graphite monochromated Mo Kα-radiation ($\lambda = 0.71070$ Å). Data integration was carried out using the CrystalClear software package (Rigaku). The structure was solved by direct methods and refined using CrystalStructure crystallographic software package (Rikagu and Rikagu.MSC). The powder pattern calculation was performed using Mercury CSD (CCDC, Cambridge, UK). The morphologies of crystals were analyzed using an Olympus BX51 polarized light microscope. TGA was carried out using a SDT2960 simultaneous DSC−TGA (TA Instruments Co. Ltd.). Approximately 6.50 mg of each sample was added to an aluminum crucible, and the accurate weight was recorded. The samples were heated over the temperature range of 25–250 °C at a constant heating rate of 5 °C/min with a purge gas of nitrogen at a flow rate of 200 mL/min. DSC measurements were performed using a Perkin-Elmer diamond DSC (Perkin-Elmer, Beaconsfield, UK). The samples (2–5 mg) were placed in sealed aluminum pans (with holes) under nitrogen purge at a flow rate of 20 mL/min, and heated from 40 to 240 °C at a scanning rate of 100 °C/min. Water contents in solution samples were measured using an 831 KF Coulometer (Metrohm, Switzerland).

Results and Discussion

The experimental PXRD patterns of CBZA and CBZD prepared are compared with the patterns simulated from the crystal structures. In Figure 3, the characteristic high-intensity diffraction peaks (2θ) of the PXRD pattern of CBZA lie at 10.26, 13.04, and 15.85, and this pattern agrees with the

(12) Brodie, M. J.; Dichter, M. A. *N. Engl. J. Med.* **1996**, *334*, 168–175.
(13) Edwards, A. D.; Shekunov, B. Y.; Forbes, R. T.; Grossmann, J. G.; York, P. *J. Pharm. Sci.* **2001**, *90*, 1106–1114.
(14) Gelbrich, T.; Hursthouse, M. B. *CrystEngComm* **2006**, *8*, 448–460.
(15) Hilfiker, R.; Berghausen, J.; Blatter, F.; Burkhard, A.; De Paul, S. M.; Freiermuth, B.; Geoffroy, A.; Hofmeier, U.; Marcolli, C.; Siebenhaar, B.; Szelagiewicz, M.; Vit, A.; von Raumer, M. *J. Therm. Anal. Calorim.* **2003**, *73*, 429–440.
(16) McMahon, L. E.; Timmins, P.; Williams, A. C.; York, P. *J. Pharm. Sci.* **1996**, *85*, 1064–1069.
(17) Laine, E.; Tuominen, V.; Ilvessalo, P.; Kahela, P. *Int. J. Pharm.* **1984**, *20*, 307–314.
(18) Tian, F.; Zeitler, J. A.; Strachan, C. J.; Saville, D. J.; Gordon, K. C.; Rades, T. *J. Pharm. Biomed. Anal.* **2006**, *40*, 271–280.
(19) Young, W. W. L.; Suryanarayanan, R. *J. Pharm. Sci.* **1991**, *80*, 496–500.
(20) Qu, H.; Louhi-Kultanen, M.; Kallas, J. *Int. J. Pharm.* **2006**, *321*, 101–107.

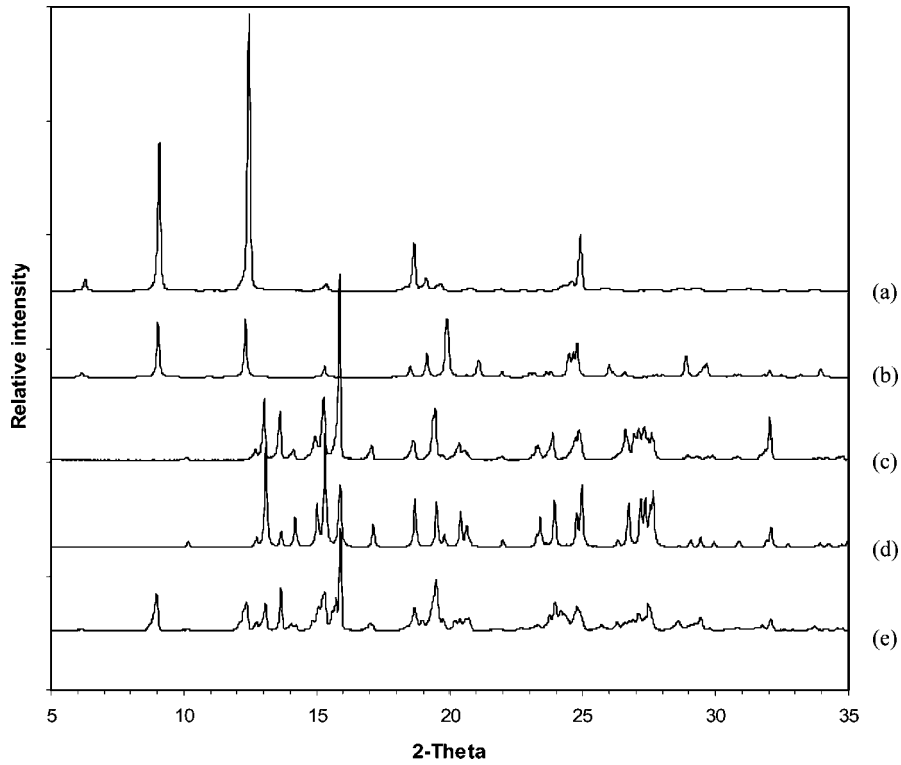

Figure 3. **PXRD patterns of CBZA and CBZD. (a) Experimental pattern of CBZD, (b) simulated pattern of CBZD, (c) experimental pattern of CBZA, (d) simulated pattern of CBZA, (e) experimental pattern of mixture of CBZA and CBZD obtained on the third day of slurry experiment.**

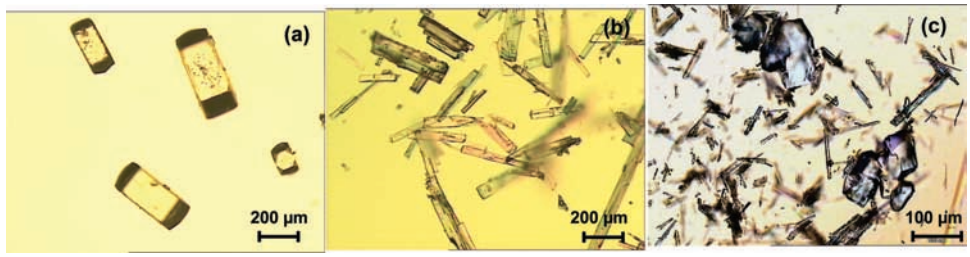

Figure 4. **Microscopic image of CBZA and CBZD. (a) Pure CBZA, (b) pure CBZD, and (c) mixture of CBZA and CBZD obtained on the third day of slurry experiments.**

simulation result and the published data.[20,21] The characteristic high-intensity diffraction peaks (2θ) of the PXRD pattern of CBZD lie at 9.09, 12.46, and 18.68. There are noticeable differences between the experimental and simulated patterns of CBZD, especially from 18° 2θ onwards. In order to confirm that our obtained CBZD sample is not contaminated with other polymorphs of CBZ, the experimental pattern was compared with the simulated patterns of all known polymorphs of CBZ available from the Cambridge Structural Database (CSD), and it matches with none of the known polymorphs of CBZ. Single crystals of CBZD were also grown in our laboratory and analyzed using SCXRD. The single crystal structure solved agreed with that available from CSD refcode FEFNOT02. However, upon grinding the single crystals for PXRD analysis, the experimental PXRD pattern obtained was identical to our original experimental pattern shown in Figure 3a. We believe that the discrepancies between simulated and experimental PXRD pattern of CBZ could stem from multiple microtwinning in the CBZD crystals as mentioned in the original reference of FEFNOT02.[22] This raises the possibility of a family of structures of CBZD containing various amounts of microtwinning especially after grinding. This is a subject for further study, but it is beyond the scope of this paper. Nevertheless, our experimental PXRD pattern of CBZD agrees well with the experimental patterns reported by various researchers.[18,20,23–25] Therefore, we believe that our CBZD samples are pure and not contaminated by other polymorphs.

Figure 4 shows the typical morphologies of CBZA and CBZD. CBZA is prismatic, whereas CBZD is platelike. As morphological differences between CBZA and CBZD are significant, morphology is a good indicator for detecting different forms.

The DSC trace of CBZA in Figure 5a shows two endothermic peaks and a concurrent exothermic peak, which is in

(21) Grzesiak, A. L.; Lang, M. D.; Kim, K.; Matzger, A. J. *J. Pharm. Sci.* **2003**, *92*, 2260–2271.
(22) Harris, R. K.; Ghi, P. Y.; Puschmann, H.; Apperley, D. C.; Griesser, U. J.; Hammond, R. B.; Ma, C. Y.; Roberts, K. J.; Pearce, G. J.; Yates, J. R.; Pickard, C. J. *Org. Process Res. Dev.* **2005**, *9*, 902–910.
(23) Wyttenbach, N.; Alsenz, J.; Grassmann, O. *Pharm. Res.* **2007**, *24*, 888–898.
(24) Kobayashi, Y.; Ito, S.; Itai, S.; Yamamoto, K. *Int. J. Pharm.* **2000**, *193*, 137–146.
(25) Han, J.; Suryanarayanan, R. *Int. J. Pharm.* **1997**, *157*, 209–218.

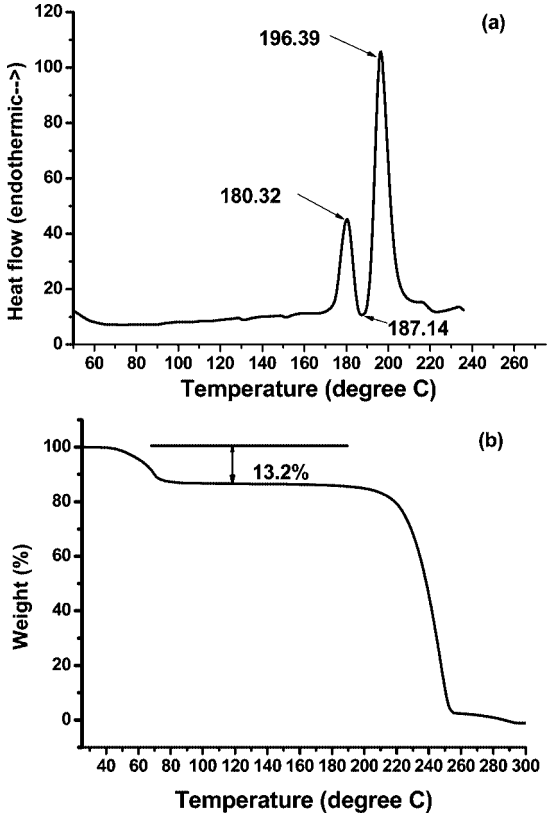

Figure 5. **(a) DSC trace of CBZA and (b) TGA curve of CBZD.**

agreement with the literature data.[26] The first peak corresponds to the melting of CBZA (180.32 °C), followed by exothermic crystallization of high temperature stable form (triclinic) at 187.14 °C, which subsequently melted at 196.39 °C. The TGA curve for CBZD in Figure 5b suggests that CBZD dehydrates when heating at 48−80 °C, and the weight percentage of water in CBZD is 13.2%, which is in good agreement with the predicted value (13.23%) from the stoichiometry of CBZD.

Thus, through the above detailed characterizations, it is confirmed that CBZA and CBZD prepared are consistent with previous literature results and are of very high purity.

In the slurry experiments, CBZA, CBZD, and their mixtures were added to an ethanol and water mixture to determine the solubility of the stable form of CBZ and the relative stabilities of the two forms. The solubility of the stable form of CBZ in ethanol–water mixtures in equilibrium are shown in conventional format in Figure 6 (see also Table 1). Ethanol is a good solvent for dissolving CBZ, while CBZ has a very low solubility in water. At 20 °C, when the water content of the solvent mixture in equilibrium (C_{we}) is lower than 19.6%, CBZA is the stable solid form in equilibrium with the saturated solution. In contrast, CBZD is the stable solid form when C_{we} is higher than 19.6%. When C_{we} is equal to 19.6%, mixtures of CBZA and CBZD coexist with the saturated solution. The mixture of CBZA and CBZD obtained on the third day of slurry experiments is characterized by PXRD (Figure 3e) and microscopy (Figure 4c). The results of the PXRD pattern and the microscopic image demonstrate that the solid sample obtained at such

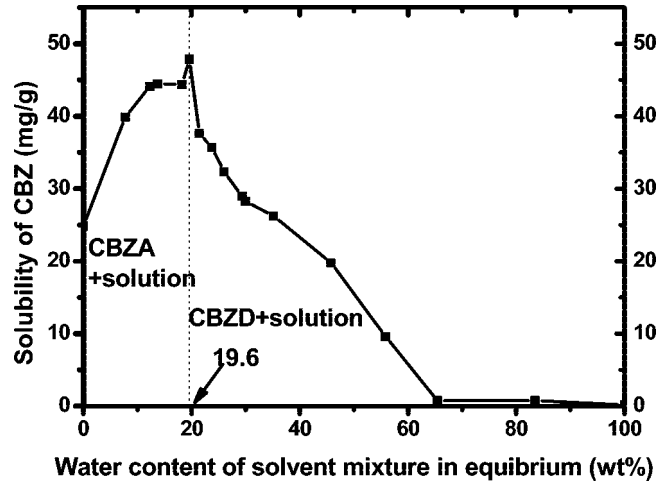

Figure 6. **Solubility profile of the stable form of CBZ as a function of water content in water−ethanol mixture at 20 °C.**

Table 1. **Solubility of CBZ in water−ethanol mixture and the equilibrium solid form**

water content of solvent mixture in equilibrium (wt%)	water activity by calculation	solubility of CBZ(mg/g solvent)	stable form
0.00	0.000	24.85	CBZA
7.77	0.370	39.90	CBZA
12.32	0.507	44.14	CBZA
13.73	0.539	44.50	CBZA
18.25	0.618	44.41	CBZA
19.57	0.636	47.90	CBZA+CBZD
21.47	0.658	37.61	CBZD
23.74	0.680	35.68	CBZD
25.98	0.698	32.35	CBZD
29.35	0.721	28.98	CBZD
29.96	0.725	28.28	CBZD
35.15	0.751	26.23	CBZD
45.75	0.794	19.81	CBZD
55.85	0.831	9.59	CBZD
65.49	0.866	0.73	CBZD
83.50	0.935	0.77	CBZD
100.00	1.000	0.13	CBZD

conditions is the physical mixture of CBZA and CBZD. In order to further confirm whether the mixture of CBZA and CBZD has reached thermodynamic equilibrium, solid samples in the slurry experiment were collected on the 7th and 14th days, and the PXRD patterns of the samples were measured (the results are not shown). It was found that the PXRD patterns of the mixture on the 7th and 14th days were almost the same as that obtained on the third day. This confirms that the mixture of CBZA and CBZD obtained at C_{we} = 19.6% was in thermodynamic equilibrium, and this means that CBZA and CBZD have the same stability at this system composition.

From the solubility curve, it is found that the total solubility of CBZA and CBZD at C_{we} = 19.6% is higher than that in pure water and ethanol. Moreover, there is a maximum in the CBZ solubility versus solvent composition (water content in solvent mixture), and this maximum occurs at the boundary between zones where different forms (CBZA and CBZD) are obtained. This observation is consistent with the literature results previously reported for the same system.[20] Solubility maxima coinciding with a transition between hydrate and anhydrate have

(26) McGregor, C.; Saunders, M. H.; Buckton, G.; Saklatvala, R. D. *Thermochim. Acta* **2004**, *417*, 231–237.

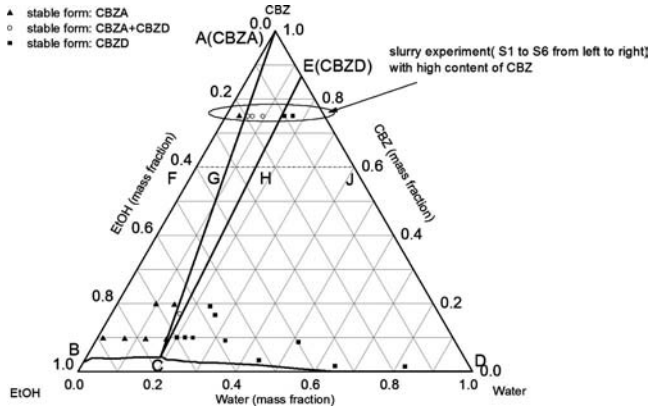

Figure 7. **Three-component phase diagram of CBZ−ethanol–water at 20 °C.**

also been reported for other systems, e.g., cholesterol,[27] cephaloglycine, cephalexin,[28] and an active pharmaceutical ingredient.[11] However, an exception to such general phenomena has been reported for theophylline in several binary aqueous cosolvent systems.[7,29]

One disadvantage of displaying solubility data for three-component systems conventionally as shown in Figure 6 is that the system composition is not clear. An isothermal triangular phase diagram of CBZ/ethanol/water at 20 °C is constructed in Figure 7 for better understanding of the relative stability of CBZA and CBZD. In Figure 7, the stable solid form of each experiment is labeled as different symbols (triangle for CBZA, circle for CBZA+CBZD, and square for CBZD). Points A, B, D, and E in Figure 7 represent CBZ anhydrous form (CBZA), solubility of CBZ in ethanol, solubility of CBZ in water, and CBZ dihydrate (CBZD), respectively. BCD is the solubility curve of CBZ in ethanol–water mixture, and below the solubility curve CBZ is completely dissolved in ethanol–water. When the system composition is located in the triangle region ABC, the stable form equilibrated with saturated solution is CBZA; while when the system composition is located in the triangle region CDE, the stable form in equilibrium with saturated solution is CBZD. The triangle region ACE represents the range of system compositions at which CBZA and CBZD can coexist in equilibrium.

From Figure 7, it can be seen that the coexistence region of CBZA and CBZD varies significantly with CBZ content. A dotted line *FGHJ* is drawn in Figure 7 as an example to show the range of coexistence region in which CBZ content is 60%, and Points G and H represent the low and high limitations of water content in the coexistence region. The predicted range of water content of the coexistence region varying with the CBZ content is illustrated in Table 2. When the CBZ content is as low as 10%, the coexistence region is quite narrow. When the CBZ content is 80%, the range of water content of coexistence region is up to 9.77%. Generally, as CBZ content increases, the coexistence region becomes wider, and the opportunity of detecting the mixture of CBZA and CBZD in equilibrium becomes higher. In order to validate this reasoning, slurry experiments with high CBZ content were conducted, and the system composition and stable solid form obtained in equilibrium are shown in Table 3. After mapping the experimental results on the phase diagram, we found that the stable form obtained in the slurry experiment is consistent with that predicted by the phase diagram.

Table 2. **Range of water content in the coexisting region in which CBZA and CBZD are in equilibrium**

CBZ content (wt %)	low limitation of water content (wt %)	high limitation of water content (wt %)	range of water content (wt %)
10	17.48	18.18	0.70
20	15.54	17.40	1.86
40	11.64	16.05	4.41
60	7.84	15.04	7.20
75	4.73	13.80	9.07
80	3.94	13.71	9.77

Table 3. **Slurry experiments with high CBZ content**

experiment	water (wt %)	CBZ (wt %)	ethanol (wt %)	stable form
S1	3.4	75.0	21.6	CBZA
S2	5.6	75.0	19.4	CBZA+CBZD
S3	6.8	75.0	18.2	CBZA+CBZD
S4	9.4	75.0	15.6	CBZA+CBZD
S5	14.9	75.0	10.1	CBZD
S6	17.0	75.0	8.0	CBZD

According to the previous studies,[7,8,11] it is found that water activity is the key factor in determining the relative stability of anhydrate and hydrate in solvent mixture. The formation of CBZD from CBZA can be represented by the following equilibrium.

$$\mathrm{CBZA} + 2\mathrm{H_2O} \rightleftharpoons \mathrm{CBZD}$$

$$K_h = \frac{a[\mathrm{CBZD}]}{a[\mathrm{CBZA}]a_w^{\,2}} \tag{5}$$

where K_h is the equilibrium constant for the hydration reaction, and a[CBZA], a[CBZD], and a_w are the thermodynamic activities of CBZA, CBZD, and water respectively. If the pure solids of anhydrate and hydrate are taken as the standard states, then the thermodynamic activities of solids (a[CBZA] and a[CBZD]) are equal to one, eq 5 can be simplified as below:

$$K_h = a_w^{\,-2} \tag{6}$$

It is also known that the low concentrations of dissolved organic compounds have little influence on the water activity in water−solvent system.[7,8] Ignoring the influence of dissolved CBZ on the water activity, the value of water activity coefficient

(27) Bogardus, J. B. *J. Pharm. Sci.* **1982**, *71*, 370–372.
(28) Pfeiffer, R. R.; Yan, K. S.; Tucker, M. A *J. Pharm. Sci.* **1970**, *59*, 1809–1814.
(29) Gould, P. L.; Howard, J. R.; Oldershaw, G. A. *Int. J. Pharm.* **1989**, *51*, 195–202.

in solvent mixture in equilibrium are calculated using eq 7 which was derived using data from the literature[30] and the Margules' formula.[31]

$$\ln \gamma_{water} = 1.425x^2_{ETH} + 0.616x^3_{ETH} - 1.248x^4_{ETH} \quad (7)$$

where γ_{water} is the activity coefficient of water and x_{ETH} is the mole fraction of ethanol in the solution. The values of water activity calculated are shown in Table 1.

When CBZA and CBZD are in equilibrium, K_h can be calculated by eq 5. Table 1 shows that, when $a_w = 0.636$, CBZA is in equilibrium with the CBZD. Therefore, $K_h = 0.636^{-2} = 2.47$. When $a_w > 0.636$, CBZD is more stable than CBZA. When $a_w < 0.636$, CBZA is more stable than CBZD. Previous workers[20,32] reported $a_w = 0.601$ at 20 °C. In the work of Qu et al.,[20,32] solubility was measured in the presence of excess solid, with the amount of excess solid not reported. Where the solid has transformed to the dihydrate, this water will have been extracted from the solution, and the solution composition will have been altered by an extent dependent on the amount of solid present. The water content in the solution will thus be different from the initial starting solution. The water activity calculated on the basis of the composition of the initial starting solution will not be the actual value of the solution at equilibrium. In contrast, in this work, the water content in the solution was measured after equilibration, and this may explain the discrepancy between the previously reported value of a_w and the value obtained in this work. This emphasizes the need to distinguish carefully between solution and system composition.

Further slurry tests were performed to investigate if the equilibrium water activity varies when moving across the coexistence region at the same solid content. As the purpose of this paper is to emphasize the importance of performing slurry tests in practical situations, the slurry tests were carried out in the practical solid fraction range of 0.1 to 0.2 at 20 °C. The results are shown in Table 4. It can be seen that the equilibrium water activity varies slightly in the range of 0.633−0.648. The average equilibrium water activity is around 0.638−0.641, and the percentage variation ranges from 0.6% to 1.2%. The variations are well within the limit of experimental error and the possible error associated with the use of eq 7for water activity estimation.

(30) d'Avila, S. G.; Silva, R. S. F. *J. Chem. Eng. Data* **1970**, *15*, 421–424.
(31) Prausnitz, J. M.; Lichtenthaler, R. N.; de Azevedo, E. G. *Molecular Thermodynamics of Fluid-Phase Equilibria*, 3rd ed.; Prentice Hall: NJ, 1999; p 234.
(32) Qu, H. Y.; Louhi-Kultanen, M.; Rantanen, J.; Kallas, J. *Cryst. Growth Des.* **2006**, *6*, 2053–2060.

Table 4. **Range of equilibrium water activity when CBZ anhydrate and hydrate coexist**

	equilibrium water activity when CBZA and CBZD coexist		
CBZ mass fraction	from	to	average
0.10	0.636	0.644	0.640 ± 0.004
0.15	0.633	0.648	0.641 ± 0.008
0.17	0.633	0.643	0.638 ± 0.005

Applications

Typical preparative crystallization processes operate at solute concentrations of 5–20 wt %. At these compositions, it is relatively easy to avoid undesirable system compositions at which both hydrate and anhydrate are thermodynamically stable. In comparison, the amount of solute present in crystallization experiments such as slurries, evaporative crystallizations, well-plate screens and "solvent drop" grinding can be as high as 90 wt %, giving an increased risk of forming thermodynamically stable physical mixtures of anhydrates and hydrates. Three-component phase diagrams are a useful aid to interpreting such findings correctly and linking them to observations in more dilute systems. Furthermore, by using the three-component phase diagram, the solvent composition can be adjusted so that only the desired solid form (such as anhydrate in ΔABC or hydrate in ΔCDE) is obtained at equilibrium.

Conclusion

The stability of anhydrate/hydrate of CBZ was investigated by using slurry experiments. Water contents (or water activities) play a crucial role in determining the thermodynamic stability of anhydrate and hydrate of CBZ at constant temperatures. The range of the coexistence region of CBZD and CBZA becomes wider when CBZ content increases; thus, the opportunity of detecting a mixture of CBZA and CBZD in equilibrium becomes higher. With the aid of a three-component phase diagram, the relative stabilities of CBZA and CBZD can be better understood. The coexistence phenomenon, which could be misinterpreted as a failure to reach equilibrium, can be avoided by altering solvent compositions as determined by the phase diagram.

Acknowledgment

We thank Dr. Srinivasulu Aitipamula for his help with the single crystal X-ray diffraction analysis.

Received for review June 28, 2007.

OP7001497